Separation Science and Technology
Publication details, including instructions for authors and subscription information:
http://www.informaworld.com/smpp/title~content=t713708471

Analysis of Fluidized Beds for the Simultaneous Aerosol Separation and Heat Recovery

M. M. El-Halwagi[a]
[a] Chemical Engineering Department, Auburn University, Auburn, AL

To cite this Article El-Halwagi, M. M.(1993) 'Analysis of Fluidized Beds for the Simultaneous Aerosol Separation and Heat Recovery', Separation Science and Technology, 28: 1, 855 — 872
To link to this Article: DOI: 10.1080/01496399308019524
URL: http://dx.doi.org/10.1080/01496399308019524

SEPARATION SCIENCE AND TECHNOLOGY, 28(1-3), pp. 855-872 (1993)

ANALYSIS OF FLUIDIZED BEDS FOR THE SIMULTANEOUS AEROSOL SEPARATION AND HEAT RECOVERY

M. M. El-Halwagi
Chemical Engineering Department
Auburn University
Auburn, AL 36849

ABSTRACT

A mathematical model is developed to describe the performance of fluidized beds for the simultaneous heat recovery and aerosol separation. This new concept is analyzed in light of the various transport processes taking place within the bed. A two-phase model is developed for the system in which heat and aerosol particles are transferred from the bubble phase to the emulsion phase. In addition to aerosol separation via diffusion, interception, impaction and electrostatic precipitation, thermophoretic collection is also analyzed. The results indicate that high thermal and separation efficiencies can be obtained.

INTRODUCTION

One of the primary sources of atmospheric pollution is the discharge of particulate-laden gases from chemical process industries. Owing to the recent strong emphasis on regulating industrial emissions of aerosols, there has been an increasing trend towards aerosol separation from industrial gas streams prior to their atmospheric disposal. Among the most efficient devices for aerosol separation are fluidized-bed filters in which a fluidized solid medium is used to capture the particulates.

Fluidized beds have also been used efficiently to recover energy from hot streams. These devices are called fluidized-bed heat regenerators "FBHR's". The essence of FBHR operation is the temporary storage of heat in a fluidized-solid medium.

During the past few years, several research efforts have lead to a reasonable understanding of the performance of FBHR's (1,2) and fluidized-bed aerosol filters (3). As a result of the various transport phenomena taking place when a hot particulate-laden gas is used to fluidize a solid medium, it is not difficult to envision that the fluidized bed can be designed to act as an aerosol filter and a heat regenerator simultaneously. To date, this proposed inherent characteristic of fluidized systems has not been exploited. This new concept can lead to substantial energy recovery, waste reduction and cost savings. The present work aims at developing a mathematical model that can be used to analyze the simultaneous phenomena of heat regeneration and aerosol separation in fluidized beds. The bed performance is investigated via a two-phase model which incorporates various transport processes occurring within the fluidized systems.

THEORETICAL ANALYSIS

In developing a mathematical model for the system, the following simplifying assumptions are invoked:

1. The bed can be represented by two phases; a bubble phase and an emulsion phase. Flowrate and voidage of the emulsion phase are taken as those at the minimum fluidization condition. This assumption is based on the two-phase model of Toomey and Johnstone (4) which is valid for many fluidization applications.
2. The deposition of the aerosol particles on the solid collectors does not alter the thermal properties of the collectors. This assumption is valid for

collectors whose surface areas are much larger than those of the aerosol particles and for relatively short cycle periods (few hours).

3. Physical properties of the two phases do not change spatially or dynamically. In addition, the gas is assumed to behave ideally such that its density is inversely proportional to temperatures. Therefore, the dynamics of the gas enthalpy can be neglected.
4. The bed operates adiabatically.
5. The bubbles are assumed to be uniform in size throughout the bed. Although the bubbles grow via coalescence as they rise, the assumption of a single average bubble diameter has been successfully used in modeling many fluidization applications (5).

According to the second assumption, the heat-recovery problem can be modeled independently from the aerosol separation phenomenon. In this context, the two-phase heat-regeneration model of El-Halwagi et al. (1) can be adopted. This model assumes that the bubble phase is in plug flow while the emulsion phase is completely mixed. Hence, heat balance around the emulsion phase and an element of the bubble phase can be written, respectively, as

$$W_e C_g (T_o - T_e) + H_{be} \epsilon_b A \int_o^H (T_b - T_e) dZ = M_s C_s \frac{dT_e}{dt} \tag{1}$$

$$W_b C_g dT_b + H_{be} \epsilon_b A (T_b - T_e) dZ = O. \tag{2}$$

Equation (2) can be integrated to

$$T_b - T_e = (T_o - T_e) \exp(-m_1 x). \tag{3}$$

where

$$m_1 = \frac{H_{be} \epsilon_b A H}{W_b C_g} \tag{4}$$

and

$$x = Z/H \tag{5}$$

Substituting from Eq. (3) into Eq. (1), integrating and rearranging, we get

$$T_e = T_o - (T_o - T_i)\exp(-m_2 t) \tag{6}$$

where

$$m_2 = \frac{[W_e + W_b(1 - \exp(-m_1))]C_g}{M_s C_s}. \tag{7}$$

Equation (6) describes the emulsion-phase dynamics. It can be substituted into Eq. (3) to yield

$$T_b = T_o - (T_o - T_i)[1 - \exp(-m_1 x)]\exp(-m_2 t) \tag{8}$$

which presents the transient behavior of the bubble-phase temperature profile.

The average gas temperature at height x is defined as the temperature that one would measure by sampling the gas at height x in proportion to the gas flow-rates through the two phases. Hence, Eqs. (6) and (8) can be applied at the bed outlet and combined to give the outlet gas temperature as

$$T_{gH} = T_o - (T_o - T_i)\frac{M_s C_s m_2}{W C_g}\exp(-m_2 t). \tag{9}$$

Having presented the dynamics of the outlet-gas temperature, one can next derive an expression for the thermal-recovery efficiency. The efficiency of heat recovery from a hot gas during a certain time period, t_r, may be defined as (6):

$$\begin{aligned} \eta_r &= \frac{\textit{heat taken up by cold solids in time } t_r}{\textit{maximum possible heat gain in time } t_r} \\ &= \frac{\textit{heat lost by hot gas in time } t_r}{\textit{maximum possible heat loss in time } t_r} \\ &= Q_r / Q_{r_{max}}. \end{aligned} \tag{10}$$

The heat lost by gas in time t_r is given by

$$Q_r = \int_o^{t_r} WC_g(T_o - T_{gH})dt. \tag{11}$$

Substituting for T_{gH} from Eq. (9) into Eq. (11) and integrating, we obtain

$$Q_r = M_sC_s(T_o - T_i)[1 - \exp(-m_2t_r)]. \tag{12}$$

The maximum possible heat transferred in time t_r may be expressed as

$$Q_{r_{max}} = WC_g(T_o - T_i)t_r. \tag{13}$$

When Eqs. (12) and (13) are substituted into Eq. (10), we get

$$\eta_r = \frac{M_sC_s}{WC_g}\left[\frac{1 - \exp(-m_2t_r)}{t_r}\right] \tag{14}$$

which provides a description of the dynamic variation of thermal-recovery efficiency with time.

Having addressed the heat-recovery problem, we are now in a position to tackle the aerosol-separation phenomenon. Owing to the axial and dynamic variations of temperature, a numerical algorithm is needed. Hence, the bed is divided into a number of compartments (stages) in series. Each stage consists of an emulsion phase and a bubble phase; each of which is assumed to be completely mixed. The height of each stage is taken as the average bubble diameter of the bed. Therefore, unlike the heat-transfer model, the mixing patterns for aerosol separation will be described via a stagewise model. This model, which is equivalent to an axial dispersion representation, is appropriate for describing aerosol separation (3). In addition to bubble-emulsion interphase transfer of the aerosol particles via convection/diffusion (7), they can be also transported via thermophoresis induced by the temperature gradient between the two phases. Furthermore, aerosol collection within the emulsion phase can be accomplished through Brownian diffusion, direct interception, inertial impaction and electrostatic forces. As has been indicated in modeling the heat-transfer operation, the bubble-emulsion temperature gradient changes dynamically. Hence, the rate of interphase transfer of aerosols due to thermophoresis also changes dynamically. Therefore, material balance equations ought to be applied for each time discretely. At a given time t, material balance equations for the aerosol particles around the n^{th} stage of the bubble phase and the emulsion phase are given, respectively, by

$$U_b C_{b,n-1} - U_b C_{b,n} - K_{be}\epsilon_b(C_{b,n} - C_{e,n})\Delta Z - K_t C_{b,n} = O \tag{15}$$

and

$$\begin{aligned} U_{mf}\, C_{e,n-1} - U_{mf} C_{e,n} + K_{be}\epsilon_b(C_{b,n} - C_{e,n})\Delta Z + K_t C_{b,n} \\ - U_{mf}\eta_e\left[\frac{1.5(1-\epsilon_{mf})}{d_c}\right](1-\epsilon_b)\Delta Z C_{e,n} = O. \end{aligned} \tag{16}$$

The following boundary conditions can be used:

$$C_{b,o} = C_o \tag{17}$$

and

$$C_{e,o} = C_o. \tag{18}$$

Equations (15) and (16) can be solved simultaneously for each stage to yield $C_{b,n}$ and $C_{e,n}$. The average aerosol concentration leaving the bed is given by

$$\overline{C_N} = (U_b C_{b,N} + U_{mf} C_{e,N})/U \tag{19}$$

and the overall collection efficiency is expressed as

$$E = 1 - \frac{\overline{C_N}}{C_o}. \tag{20}$$

Having derived a complete model for the system, it is necessary to outline expressions for evaluating the model parameters. These are given in the Appendix. For a given operating time, the solution procedure is carried out as follows. First, Eqs. (6) and (8) are used to evaluate the temperatures of the bubble and the emulsion phases throughout the bed. Equation (14) is then employed to evaluate the thermal efficiency of the bed. Having identified temperature gradients throughout the bed, Eqs. (15) and (16) are solved simultaneously for each stage to calculate the concentration of aerosols in the bubble and the emulsion phases. The computation is carried out till the uppermost stage is reached. Hence, Eq. (20) is used to calculate overall collection efficiency. In the sequel, the model is used to investigate the behavior of the proposed system for simultaneous heat recovery and aerosol separation.

RESULTS AND DISCUSSION

In order to analyze the performance of fluidized beds for the simultaneous aerosol separation and heat recovery, the proposed model is used to estimate the dynamic performance of the sytem. The following data are employed: T_i = 300 K, T_o = 800 K, U = 0.3 m/s, U_{mf} = 0.2 m/s, H_{mf} = 2.0 m, D_R = 1.0 m, D_c = 0.002 m and ϵ_{mf} = 0.45. Figure 1 shows the unsteady-state variation in the collector-particle temperature. As the time increases, the temperature of the solid collectors increases. Consequently, both the thermal and the collection efficiencies decrease. Figure 2 shows the dynamic reduction in the bed thermal efficiency. Owing to the continuous reduction in thermal efficiency, the bed ought to be regenerated after a reasonable period of time by temporarily passing a cold fluid instead of the hot gas. Figure 3 illustrates the dynamic variation in the collection efficiency for various aerosol-particle diameters. The nonmonotonic behavior of the aerosol-separation efficiency can be attributed to the shift from a diffusion-limited range to an impaction-limited regime. In this context, fluidized beds offer virtually complete aerosol separation for particle

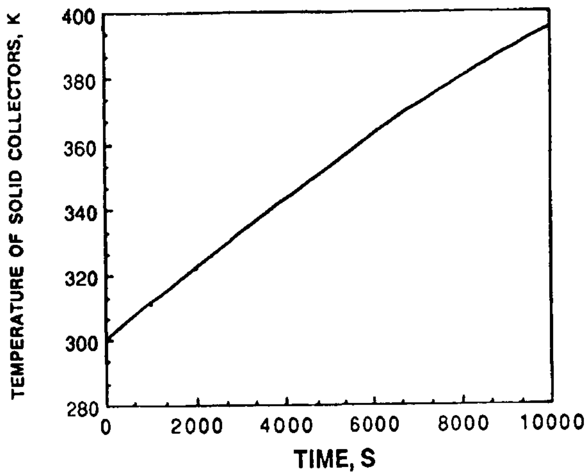

FIGURE 1. Dynamics of solid-collector temperature.

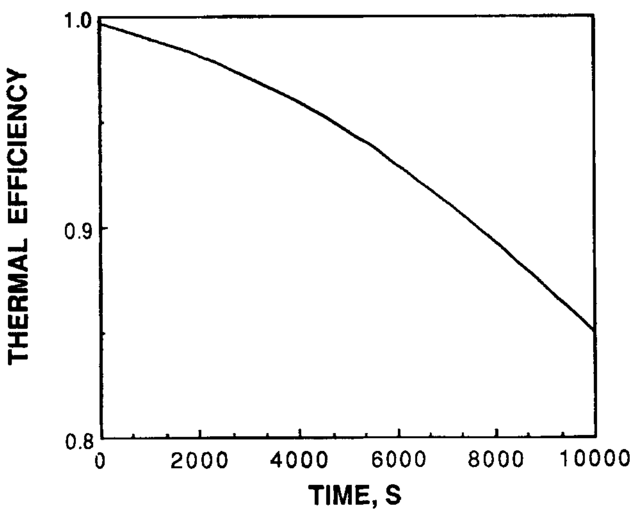

FIGURE 2. Transient thermal efficiency of the bed.

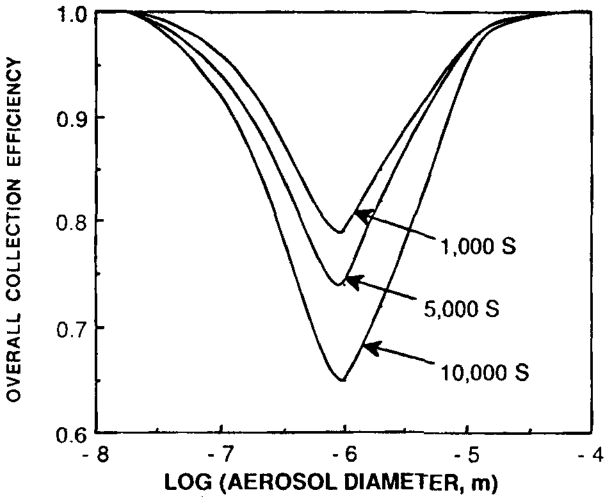

Fig. 3 Dynamics of Aerosol Collection Efficiency.

diameters smaller than 0.01 μm and larger than 100.00 μm. In the intermediate range, the collection efficiency becomes less. As time proceeds, the bubble-emulsion thermophoretic temperature gradient decreases. This leads to dynamic reduction in aerosol-separation efficiency.

CONCLUSION

A mathematical model has been developed to simulate the performance of fluidized beds for the simultaneous aerosol separation and heat recovery. A two-phase model was proposed to describe the heat- and mass-transfer phenomena throughout the bed. The model accounts for separation enhancement due to thermophoresis. The model results indicate that indeed high thermal and aerosol-separation efficiencies can be accomplished in a fluidized bed.

APPENDIX

EVALUATION OF MODEL PARAMETERS

In the following, the expressions employed in estimating the model parameters are presented. All of these parameters are related to readily-obtainable quantities.

A.1. Bubble Diameter

The correlation of Mori and Wen (8) is used to evaluate the bubble size. It is given by

$$D_b = D_{bm} - (D_{bm} - D_{bo})\exp(-0.3Z/D_R) \tag{A.1}$$

where

$$D_{bm} = 1.6377[A(U - U_{mf})]^{0.4} \tag{A.2}$$

where U is the superficial velocity of the fluidizing gas, and

$$D_{bo} = 0.376(U - U_{mf})^2 \tag{A.3}$$

(for porous distributor plates)
or

$$D_{bo} = 0.8716\left[\frac{A(U - U_{mf})}{N_D}\right]^{0.4} \tag{A.4}$$

(for perforated distributor plates with number of orifice openings = N_D).

The average bubble diameter of the bed is assumed to be the value of D_b at $H_{mf}/2$.

A.2. Fractional Volume of Bed Occupied by the Bubble Phase, ϵ_b

$$\epsilon_b = (U - U_{mf})/U_b \tag{A.5}$$

where (7)

$$U_b = U - U_{mf} + U_{br} \tag{A.6}$$

and the absolute velocity of an isolated single rising bubble as suggested by Davidson and Harrison (7) is given by

$$U_{br} = 0.711(gD_b)^{0.5} \tag{A.7}$$

A.3. The Expanded-Bed Height

The bed expansion above the height at incipient fluidization is assumed to be entirely due to the presence of bubbles, so

$$H = H_{mf}/(1 - \epsilon_b) \tag{A.8}$$

A.4. Distribution of Gas Flow Among the Phases

According to the two-phase theory of fluidization (4):

$$W_e = U_{mf}\rho_g A \tag{A.9}$$

and

$$W_b = (U - U_{mf})\rho_g A \tag{A.10}$$

or

$$U_b = U - U_{mf} \tag{A.11}$$

A.5. Interphase Exchange Coefficients

The interphase heat transfer coefficient between the bubble phase and the emulsion phase may be calculated from the following semi-empirical expression (5):

$$H_{be} = 4.5\left(\frac{U_{mf}\rho_g C_g}{D_b}\right) + 5.85\frac{(k_g\rho_g C)^{0.5}g^{0.25}}{D_b^{1.25}} \tag{A.12}$$

In a similar fashion, the bubble-emulsion interphase mass transfer coefficient is given by (7):

$$K_{be} = 4.5U_{mf}/D_b + 5.85\left(\frac{D_e^{1/2}g^{1/4}}{D_b^{5/4}}\right) \tag{A.13}$$

The thermophoretic velocity is given by (9):

$$K_t = \frac{0.4\ k_g}{(k_g + k_p)P}\ \nabla T \tag{A.14}$$

The temperature gradient can be assumed to take place linearly across the bubble clouds. Thus within the n^{th} stage

$$\nabla T \approx \frac{T_{b,n} - T_e}{\delta_n} \tag{A.15}$$

where δ_n is the n^{th} stage cloud thickness which can be estimated by (10):

$$\delta_n = D_{b,n}\left[\left(\frac{U_{br}\epsilon_{mf}/U_{mf}}{U_{br}\epsilon_{mf}/U_{mf} - 1}\right)^{1/3} - 1\right] \tag{A.16}$$

Clearly Eq. (A.15) results in a conservative estimate for the thermophoretic velocity since the actual boundary layer around the bubble occupies just a fraction of the cloud.

A.6. Single-Sphere Collection Efficiency

Aerosol filtration is assumed to take place through four collection mechanisms; Brownian diffusion, direct interception, inertial impaction, and induced electrostatic forces. The overall collection efficiencies for a single collector (η_e) is assumed to be the sum of the four mechanisms in the corresponding phase, i.e.,

$$\eta_e = \eta_D + \eta_{Int} + \eta_{Imp} + \eta_{Elect.} \tag{A.17}$$

The following expressions are used throughout this work:

Brownian diffusion (11)

$$\eta_D = 3.5\left(\frac{1 - \alpha^{5/3}}{\beta_H}\right)^{1/3} Pe^{-2/3} \tag{A.18}$$

where, Happel's (12) hydrodynamic factor is given by

$$\beta_H = 1 - 1.5\ \alpha^{0.33} + 1.5\ \alpha^{1.67} - \alpha^2. \tag{A.19}$$

Direct interception (13)

$$\eta_{Int} = \frac{1}{\beta_K}\{(1 + I)^2 - 1.5(1 + I) + \alpha[0.2/(1 + I) + 0.5(1 + I)^2 - 0.3(1 + I)]\} \tag{A.20}$$

where Kuwabara's (14) hydrodynamic factor is expressed as

$$\beta_K = 1 - 9/5\alpha^{.33} - .2\alpha^2 + \alpha. \tag{A.21}$$

Inertial impaction (15):

$$\eta_{Imp} = Stk_{eff}^{3.55}/(1.67 + Stk_{eff}^{3.55}) \tag{A.22}$$

where

$$Stk_{eff} = Stk\left[\frac{1 - \alpha^{5/3}}{1 - 1.5\alpha^{1/3} + 1.5\alpha^{5/3} - \alpha^2} + \frac{1.14Re^{1/2}}{\epsilon^{1.5}}\right]. \tag{A.23}$$

Electrostatic forces (16):

$$n_{Elect.} = \left(\frac{15\pi}{8}K_{IC}\right)^{0.4}$$

where

$$\textit{Charged-collector image force}\ K_{IC} = \frac{(\epsilon_D - 1)2CD_p^2Q_{ac}^2}{(\epsilon_D + 2)3uD_cU_{Po}\epsilon_o}.$$

NOMENCLATURE

A	cross-sectional area of bed, m^2
C	Cunningham correction factor
$C_{b,n}$	gas concentration of aerosol leaving stage n of bubble phase, $\#/m^3$

$C_{e,n}$	gas concentration of aerosol leaving stage *n* of emulsion phase, $\#/m^3$
C_g	gas specific heat, J/kg K
C_o	inlet aerosol concentration, $\#/m^3$
$\bar{C}_N$	average aerosol concentration leaving the filter, $\#/m^3$
C_s	solid-particle specific heat, J/kg K
D_b	average equivalent bubble diameter, m
D_{bm}	maximum bubble diameter, m
$D_{b,n}$	bubble size within the n^{th} stage, m
D_{bo}	initial bubble diameter, m
D_c	diameter of collector particles, m
D_e	molecular diffusion coefficient of aerosol particulates, m^2/s
D_p	diameter of aerosol particulates, *m*
D_R	bed diameter, m
E	overall aerosol-collection efficiency of the bed
g	acceleration of gravity, m^2/s
H	bed height, m
H_{be}	interphase heat exchange coefficient between bubble phase and emulsion phase (rate of heat exchanged between the bubble phase and the emulsion phase per unit time, per unit volume of bubble phase, per unit temperature difference between the bubble phase and the emulsion phase), W/m^3 K
H_{mf}	bed height at minimum fluidization conditions, m
I	interception number (D_p/D_c)
K_{be}	volumetric rate of gas exchange between bubble and emulsion phases, s^{-1}

k_g thermal conductivity of the gas, W/m K

K_{IC} dimensionless characteristic mobility for charged-collector image force

k_p thermal conductivity of the aerosol particles, $\frac{W}{mK}$

K_t thermophoretic velocity, m/s

m_1 dimensionless parameter given by Eq. (4)

m_2 defined by Eq. (7), s^{-1}

M_s total mass of solid particles inside the bed, kg

N total number of stages in bed

N_D number of orifice openings on the distributor

Q_r heat lost by gas or heat uptaken by solids, J

$Q_{r_{max}}$ maximum possible heat lost by hot gas during time t_r or maximum possible heat gained by cold solids during time t_r, J

Stk Stokes number

Stk_{eff} effective Stokes number

t time, s

t_r time during which heat is recovered from the gas by the bed, s

T_b temperature of bubble phase, K

T_{bH} outlet temperature of bubble phase, K

$T_{b,n}$ bubble-phase temperature within the n^{th} stage, K

T_e temperature of emulsion phase, K

T_g average gas temperature at height Z, K

T_{gH} outlet gas temperature, K

T_i	initial bed temperature, K
T_o	inlet gas temperature, K
U_b	absolute rise velocity of a swarm of bubbles through a fluidized bed, m/s
u_{br}	absolute rise velocity of single bubble through a fluidized bed, m/s
U	superficial velocity of gas, m/s
U_b	superficial velocity of the bubble phase, m/s
U_{mf}	superficial velocity of gas at minimum fluidization conditions, m/s
W	mass flow-rate of the gas, kg/s
W_b	mass flow-rate of bubble phase, kg/s
W_e	mass flow-rate of emulsion phase, kg/s
x	dimensionless fractional height above the distributor
Z	height above the distributor, m

GREEK SYMBOLS

α	solidity
β_H	Happel's hydrodynamic factor, Eq. (A.19)
β_K	Kuwabara's hydrodynamic factor, Eq. (A.21)
δ_n	cloud thickness within the nth stage
ΔZ	stage height, m
ϵ	fractional voidage
ϵ_b	volume fraction of bubbles in the bed
ϵ_D	dielectric constant of aerosol particulates

ϵ_{mf}	mean voidage under minimum-fluidization conditions
ϵ_O	permittivity of free space, 8.85 x 10^{-12} $C^2/N, m^2$
η_D	single spherical collection efficiency for Brownian diffusion
η_e	collection efficiency of a single sphere in the emulsion phase
η_{Elect}	single spherical collection efficiency for induced electrostatic collection
η_{ImP}	single spherical collection efficiency for impaction
η_{Int}	single spherical collection efficiency for interception
η_r	thermal efficiency of the regenerator
ρ_g	gas density, kg/m^3
ρ_s	solid density, kg/m^3

Subscripts

b	bubble phase
e	emulsion phase
n	stage number
N	final stage

REFERENCES

1. A. M. El-Halwagi, M. A. El-Rifai and M. M. El-Halwagi, Chem. Eng. Comm., 72, 121 (1988).

2. A. M. El-Halwagi, M. A. El-Rifai and M. M. El-Halwagi, Chem. Eng. Comm., 91, 235 (1990).

3. M. M. El-Halwagi, Aerosol Sci. Technol., 13, 102 (1990).

4. R. D. Toomey and H. F. Johnstone, Chem. Eng. Prog., 48, 220 (1952).

5. D. Kunii and O. Levenspiel, Fluidization Engineering, John Wiley, New York, 1969.

6. O. Levenspiel, Chem. Eng. Sci., 38 (12), 2035 (1983).

7. J. F. Davidson and D. Harrison Fluidized Particles, Cambridge University Press (1963).

8. S. Mori and C. Y. Wen, AIChE J., 21 (1), 109 (1975).

9. S. K. Friedlander, Smoke, Dust and Haze: Fundamentals of Aerosol Behavior, John Wiley & Sons, NY, 1977, p. 42.

10. R. Clift and J. R. Grace, in Fluidization, Eds. Davidson, J. F., R. Clift and D. Harrison, 2nd Ed., Academic Press, London 1985, pp. 73.

11. K. W. Lee, J. Aerosol Sci., 12, 79 (1981).

12. J. Happel, AIChE J, 4, 197 (1958).

13. K. W. Lee, and J. A. Gieseke, Envir. Sci. Technol., 13, 466 (1979).

14. S. Kuwabara, J. Phys. Soc. Jap., 14, 527 (1959).

15. T. D'Ottavio and S. L. Goren, Aerosol Sci. Technol. 2, 91 (1983).

16. H. F. Kraemer and H. F. Johnstone, Ind. Eng. Chem., 47, 2426 (1955).